

EVALUATION OF GA ESTIMATION PARAMETERS IN WIDEBAND PIEZOELECTRIC TRANSDUCERS EMPLOYING A COMPREHENSIVE MODELING TOOL

Abelardo Ruiz^(a), David K. Anthony^(a), Antonio Ramos^(a)

^(a) Dept. Ultrasonic Signals, Systems and Technology, Institute of Acoustics (CSIC),
C/ Serrano 144, 28006 Madrid. (Spain)
art@ia.cetef.csic.es, iaca344@ia.cetef.csic.es, aramos@ia.cetef.csic.es

ABSTRACT

Broadband piezoelectric transducers are used in many ultrasonic transceiver systems for Non Destructive Evaluation (NDE) and medical imaging. Precise knowledge of their internal construction parameters is required in modelling and simulation tasks to optimise behaviour in such systems. Genetic algorithms (GA) have been proposed to estimate parameters in piezoelectric backed transducers. They can help to improve the precision of the input data in the modeling and simulation tasks when this information is not available. Here, a circuit modeling approach to evaluate practical effectiveness of GA transducer estimation results, is presented and applied to achieve improvements during design and modeling tasks (with the aim of optimizing ultrasonic transceiver responses). HV spike driving and pulse-echo waveforms are simulated in time-frequency domains for selected sets of estimated parameters. Their dependences on the estimating parameters were considered, and the responses of alternative transducer designs were quantified.

Keywords: estimation parameter, genetic algorithms, transducer modeling, PSPICE simulation.

1. INTRODUCTION

Accurately determining the constructional parameters of broadband ultrasonic transducers is important in estimating the performance of pulsed transceiver systems. This type of transducer is usually involved in experimental laboratory set-ups devoted to research purposes or in the industrial context of NDE (non-destructive evaluation) of component interiors or structural materials. Often the physical internal construction details are unknown (especially for commercial probes) but parameter estimation would allow optimisation of the overall system by computer simulations based on models of the acoustic and electrical sections.

Search algorithms can be applied to estimation problems based on experimental measurements and in some cases gradient-based methods suffice. However, such methods can give misleading results if the measurements are “noisy” as can be found in ultrasonic applications of piezoelectric transducers.

A few estimation procedures for narrowband piezoelectric resonators already exist [Smits J.G., 1976.

Ruiz A., Ramos A., San Emeterio J. L., 2004] but an effective and general solution for the problems related to broadband devices is still not available. A procedure to efficiently find sufficiently approximated values of design parameters in these devices would be a valuable tool to optimise their performance in pulsed ultrasonic transceivers. This can be achieved by means of computer simulations based on models of their acoustic and electrical sections behaviours.

Additionally, black-box models for transducers were utilised in [Capineri L., Masotti L., Rinieri M., and Rocchi S., 1993, Lockwood G.R., Foster F.S., 2000] for estimation where the piezoelectric and constructional parameters were not taken into account. An artificial intelligence procedure proposed for estimation of transducer parameters in a broadband piezoelectric transmitter was presented in [Ruiz A., Ramos A., San Emeterio J. L., 2004]. Here a genetic algorithm (GA) search/optimization procedure was applied to estimate four parameters related to two pulsed transmitters whose efficiency was studied in function of the number and limits of the parameters being estimated. In this preliminary work, the GA procedure was limited by its simplicity and other values of the GA parameter were not explored.

In this paper we present a more general estimation procedure using a comprehensive application of the GA to produce transducer parameter (TP) sets. This procedure is based on an extensive combination of the GA search parameters (SP) as well as a comprehensive fitness function. A metric, the euclidean distance (ED), is used to evaluate differences between estimated transducer models resulting from several GA SP-sets. Additionally, a pulse-echo circuit modeling approach is presented in order to evaluate the effectiveness of the different TP-sets obtained from the GA when implemented in a more comprehensive transceiver model. HV spike driving and pulse-echo waveforms were simulated in time-frequency domains for selected TP-sets. The differences in performance of the TP-sets resulting from the GA are analyzed and discussed.

2. MODEL BASED FUNCTION FOR TRANSDUCER PARAMETER ASSESSMENT

A broadband piezoelectric transducer can be designed with a multi-element probe. This structure can be composed of an active element that realises the electro-

mechanic energy conversion (the piezoceramic), one or more constructive transducer elements (such as matching layers to the propagation medium) and other elements (for example, an element added to the piezoceramic back face – usually called the backing). All, or some, of these may be included in the design model depending on the specific probe application.

For successful TP estimation the proper selection of a good model should be based on an accurate knowledge of the device internal configuration, together with an adequate metric for judging the “fitness” of each solution. These are essential. Here in the estimation procedure we have employed a piezoelectric transmitter model using a thickness-mode matrix representation in frequency domain, based on the KLM transducer equivalent circuit [Krimholtz R., Leedom F., and Matthaei G., 1970], and a seven-parameter model implementation is used here.

Four parameters are estimated: Z_{0ef} and Z_{bef} (specific acoustic impedances of the piezoceramic and the backing section), h_{33} (piezoelectric constant), v_t (piezoceramic propagation velocity). The clamped piezoceramic capacity, C_0 , the nominal working frequency (f_0) and geometric area (A) have the values 1.28×10^{-9} F, 1.093 MHz and 3.14×10^{-4} m² respectively. The emitting transducer performance is represented by the emission transfer function (ETF) which is considered as a function, q , of the transducer parameters:

$$ETF(\omega) = q(Z_{0ef}, Z_{bef}, h_{33}, v_t^D, C_0, f_0, A) \quad (1)$$

Further details of the transducer model are given in [Ruíz, A., San Emeterio, J. L., Ramos, A., 2004].

3. IMPLEMENTATION OF THE GA FOR ESTIMATION

3.1. General Aspects

Genetic algorithms are stochastic-based optimisers that perform function optimisation based on the Darwinian evolution of nature [Goldberg D.E., 1989]. In general, they are applied to search spaces that are too large to be exhaustively searched or are used when the search space is multi-modal or discontinuous. Each set of TP (that define a possible solution) is coded in the form of a finite length binary “chromosome” string. Each different chromosome corresponds to a unique set of TP values. The GA is initialised with a random pool of chromosomes and consecutive generations are obtained involving to three key operations: selection, crossover and mutation. The average fitness of the generations successively increases and the process is halted after a number of generations by a suitable convergence criterion. Using an *elitist* strategy, the best-so-far solution is guaranteed to survive into the next generation.

When applying GAs, it can never normally be established whether the true global optimal solution has been found. Consecutive applications of the algorithm

lead to near-optimal solutions and in most cases these out perform the existing design, and seeking the true globally optimum design is often not a necessity. A more complete description of GAs can be found in [Goldberg D.E., 1989].

As GAs rely on random numbers in its operation, the result will depend upon the start seed of the random number generator as well as of the GA SP.

3.2. The GA implementation

The success of the GA results depends on how representative the objective (or fitness) function is. It is the sum of the ‘fit’ between the normalised moduli and the error in the real part of the electrical input impedance, and is

$$F = \frac{1}{N} \sum_{i=1}^N \left[\left(|ETF(\omega)|_{N_i}^{\text{exp}} - |ETF(\omega)|_{N_i}^{\text{est}} \right)^2 + k * \left((MR_{\text{exp}} - MR_{\text{est}}) / MR_{\text{exp}} \right)^2 \right] \quad (2)$$

$|ETF(\omega)|_{N_i}^{\text{exp}}$ is the normalised modulus of the experimental curve and $|ETF(\omega)|_{N_i}^{\text{est}}$ is the normalised modulus of the estimated curve (from the model), where j is an index for each generation being evaluated. The normalization process is governed by N_j that is calculated for each generation, and applied to this same generation. This is now described.

For the first generation, the response $|ETF(\omega)|_{N_1}^{\text{exp}}$ is calculated for each TP-set in first generation. N_1 is the maximum value over the whole generation. In subsequent generations, N_j , is calculated similarly except the *minimum* value is evaluated.

MR_{exp} and MR_{est} are the maximum values of the real part of the impedance at the frequency of maximum resistance f_p , $\text{Re}\{Z_{\text{in}}(f_p)\}$, for the experimental and GA evaluated responses. In (2), N is the number of samples in the ETF curves and k is an empirical factor introduced to regulate the influence of the second term. The GA was configured to minimise F .

The GA was implemented in MATLAB. The values of the 4 parameters (Z_{0ef} , Z_{bef} , v_t^D , h_{33}) were limited to specific ranges and coded as a binary chromosome of total length of 83 bits. The initial generation is randomly assigned. As the GA is a stochastic search algorithm its performance is dependent on the GA parameters (SP) as well as the start seed of the random number generator. So as to apply the GA in a way that does not produce results specific the SPs and the random seed number 1350 GAs were run with different combinations of SPs and start seeds.

Three values of generation size (*ncrom*) and total number of generations (*ngen*) were used each having a constant number of objective function evaluations: $ncrom/ngen = \{40/50, 100/20, 200/10\}$.

Roulette wheel selection was used in conjunction with different conditioning operations (reciprocal, linear

inversion, and linear inversion with translation to zero) and scaling functions (no scaling, rank selection, Sigma scaling and logarithmic scaling). The scaling functions convert the smaller better value of the objective function to larger sections on the circumference of the roulette wheel. The scaling functions relate how much better a better solution is (e.g. on linear or logarithmic terms, for example). It is noted that when using rank selection the results are independent of the conditioning function.

Three values of crossover and mutation probability were used, $p_c = \{0.6, 0.75, 0.9\}$ and $p_m = \{0.5, 1, 2\}/ncrom$. A second crossover point was performed with a probability of 0.5 allowing both single- and double-point crossovers so that the performance of the GA is less dependent upon the order of the parameters within the chromosome.

The 1350 GA runs when processed on a desktop PC (Intel Pentium 4, 2.40 GHz) took approximately 7 hours. It is noted that there are a total of approximately 10^{25} solutions (for a 83 bit chromosome) and so an exhaustive search is not feasible (requiring more than 10^{20} years). Otherwise, methods of efficiently sampling the full combinational GA parameter set would have to be used.

4. EUCLIDEAN DISTANCE ANALYSIS

The 1350 GAs produce solutions (TP-sets) that give optimal performance (good transducer estimation). Relatively small variation in performance is seen. However, a wider variation is seen in the TP-sets. The Euclidean distance (ED) was used as a metric to measure the distinctness between TP-sets, effectively indicating the difference in the resulting transducer design. This is not the same as differences in the value of their objective functions (i.e., the performance). Using the ED, transducer designs that are distinct can be sought and the differences between them studied.

For M -parameter model the ED between two solutions, r and s , is calculated from the normalised differences in each parameter, m , denoted as $a_m(r)$ and $a_m(s)$, and is

$$ED(r, s) = \sqrt{\frac{1}{M} \sum_m \left(\frac{a_m(r) - a_m(s)}{a_{m,max} - a_{m,min}} \right)^2} \quad (3)$$

$a_{m,min}$ and $a_{m,max}$ are the minimum and maximum values of parameter m used in the GA. The ED measure has the range $\{0,1\}$.

Z_{0ef}	Z_{bef}	h_{33}	v_t^D	F	ED	SP-set
3.41E6	3.69E7	1.92E9	4036	5.6E-1	.232	BS
2.53E6	2.89E7	1.72E9	3615	7.9E-1		AS

Table 1. TP-sets, F and ED values of BS and AS.

The EDs between the TP-sets resulting from the 1350 SP-sets were calculated. This enables many different cases to be studied but here only one is presented. The best overall TP-set (denoted BS) (with

the lowest value of F) was compared with another TP-set (denoted AS) having a very similar value of F but with distinct TPs. In this case the ED was greater than 0.2. Table 1 shows TPs and values of F for the two transducer designs.

5. EVALUATING THE EFFECTIVENESS OF THE GA ESTIMATION USING A CIRCUITAL PULSE-ECHO MODEL

A circuitual pulse-echo (P-E) model was employed in order to evaluate by simulation the effectiveness of the GA estimation procedure [A. Ruíz, M. Hernández, A. Jiménez, A. Sotomayor, O. Sánchez, A. Ramos, P. T. Sanz, J. L. San Emeterio, 2002]. This emitting-receiving arrangement was implemented in PSPICE [OrCADTM]. Figure 1 presents the circuit diagram of the wideband P-E arrangement used.

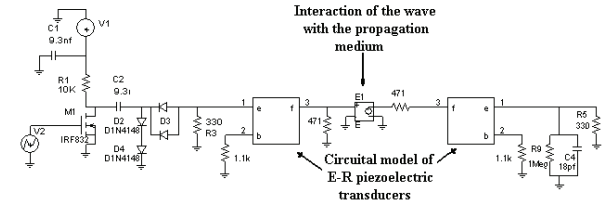


Figure 1: Electrical diagram of the ultrasonic Pulse-Echo arrangement.

The emitter and receiver (E-R) transducers are represented by identical three-port blocks based on a Redwood equivalent circuit [Redwood M., 1961]. These included a quadratic frequency dependence of the mechanical losses in the piezoceramic material [Ramos A., Ruíz A., San Emeterio J. L., Sanz P.T., 2006]. The emitter and receiver blocks represent the two functions (transmit and receive) of one physical transducer separately and have identical geometric and piezoelectric parameters. Pin “e” represents the electrical port, and “b” and “f” denote the back and front mechanical ports of the probes.

The electronic driving stage was modelled by a simplified configuration of a pulsed generator circuit as those employed in NDE. The receiving stage effects were considered by means of a simplified receiver input impedance. Some aspects of the input impedance of the oscilloscope and a damping resistor of the driving structure were included. The resistor is a first approximation of the excitation circuit effects in the echographic signal.

Block E1 represents a dependent voltage source which electrically decouples both piezoelectric stages. From the acoustical point of view E1 models (in a very simplified way) the interaction of the acoustic wave with the propagation medium. The basic gain, β , of E1 can be expressed by the following equation:

$$\beta = 2 e^{-\alpha x} \left(\frac{Z2 - Z1}{Z2 + Z1} \right) \quad (4)$$

where α is the attenuation coefficient of the propagating wave and x is the distance travelled by the wave in the

propagation medium. The fraction in equation (4) is the reflection coefficient at the interface reflector material - propagation medium, where Z_1 and Z_2 are the acoustic impedance of the propagation medium and reflector material respectively.

With minor changes, the circuit diagram in Figure 1 can be also employed to model Through - Transmission (T-T) responses. In this case, the ratio between the geometric areas of the receiver and emitter transducers must be introduced in (4). Additionally, an inductive matching component can also be included in the emitting -receiving electronic to model other T-T cases.

6. RESULTS

6.1. From the GA estimation procedure and the Euclidean distance employment

Figure 2a) shows a comparison between the experimental (in blue) and two estimated curves of the normalized modulus of the ETF for an estimation process of four parameters. The black curve represents the *BS* taking into account the equation (2). The green curve was obtained for the TP-set *AS*. All curves have been normalized because the fitness function is based on the shape of the ETF modulus and $\text{Re}\{Z_{in}(f_p)\}$, where this last curve takes account of the amplitude aspects.

From the transducer estimated parameters, the electrical impedance has been computed and the real part of this transducer characteristic function is presented in Figure 3b). A reasonably good agreement can be appreciated in all the curves shown in Figure 3. Nevertheless, the *BS* has better agreement with $\text{Re}\{Z_{in}\}$ than *AS*, although the difference is small.

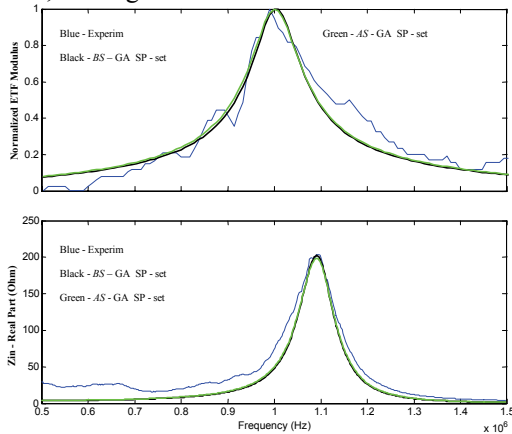


Figure 2: Comparison between the experimental and two GA estimated curves versus the frequency: a) Normalized Modulus of the ETF b) Real part of the electrical input impedance.

Here, only $\text{Re}\{Z_{in}\}$ is shown because this is more directly related with the second term of the fitness function used in this work. However, it is noted that the imaginary part of the computed Z_{in} also has reasonably good agreement with the experimental curve but is not presented here.

6.2. Employment of the circuitual modeling approach

Based on the configuration presented in Figure 1 simulated P-E results were obtained for a reflection of the emitted ultrasonic pulse in an interface water/plastic located at a near-field distance of 50 mm from the transducer front face. The reflector material considered was PMMA (with a specific acoustic impedance, Z_{PMMA} , of 3.2 MRayls).

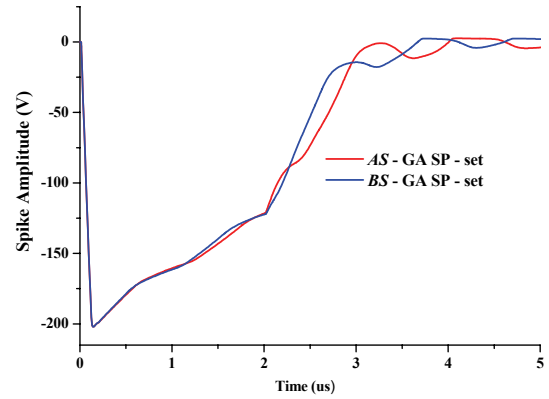


Figure 3: Driving responses for the P-E configuration with a piezoceramic transducer modelled from TP sets obtained from two different GA SP-sets: Blue: *BS* - SP-set. Red: *AS* - SP-set.

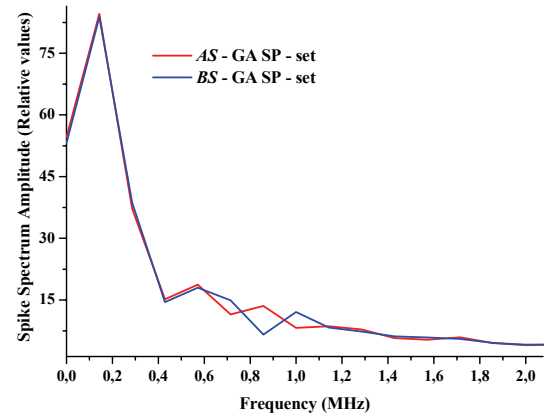


Figure 4: Driving frequency spectra for the pulse-echo configuration involving a piezoceramic transducer modelled with TP-sets obtained from two different GA SP-sets: Blue: *BS* - GA SP-set. Red: *AS*-GA SP- set.

Figure 3, presents the simulated driving temporal responses for the P-E configuration for a piezoceramic transducer modelled with TP-sets obtained from *BS* and *AS* SP-sets. A slightly shorter rise time for the *AS* TP-set can be seen. Additionally, there are certain distortions in the spike waveforms that are induced from the motional behavior of the piezoelectric loads. These are more clearly appreciated for *AS*. The differences in both simulated signals can be influenced

by the different values of the estimated impedances associated to every transducer (see Table 1) [Ramos A., San Emeterio J. L., Sanz P.T, 2000].

In Figure 4, a comparison of the driving frequency spectra for the P-E configuration with a piezoceramic transducer modelled with *BS* and *AS* TP-sets is made. Here, the colors of the curves are the same as those in Figure 3. The behaviour of the spike waveforms is very similar, especially at low frequencies. Nevertheless, in the frequency range of interest to ultrasonic responses (0.5-1.5 MHz), some notable differences between both curves can be appreciated.

Two simulated pulse-echo waveforms obtained with *BS* and *AS* TP-sets are shown in Figure 5. The blue line shows the results obtained with the *BS* TP-set. The red line shows the results with the *AS* TP-set. There is a notable difference between the amplitudes of both waveforms, as well as a small difference in the resonance frequency. These disagreements can be caused by the difference of some of the estimated transducer parameters, among which is the longitudinal wave propagation velocity in the piezoceramic which directly influences the transducer frequency. On the other hand, the temporal pulse length is shorter for the *BS* option. This can be explained by the higher value of Z_b than the *AS* TP-set.

A comparison of the pulse-echo frequency responses associated with the curves presented in Figure 5, is shown in Figure 6. The frequency shifting can be more clearly appreciated in the resonance peaks of the second harmonic.

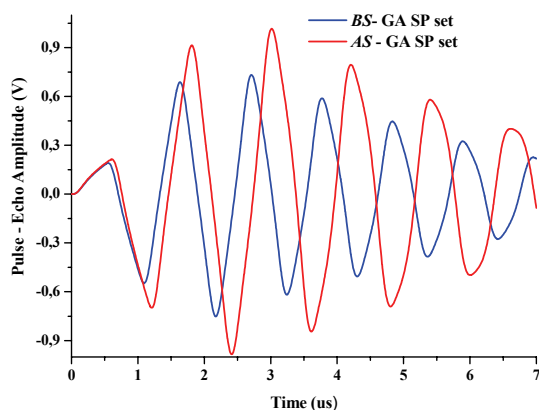


Figure 5. Simulated pulse-echo temporal responses. Blue color: *BS* GA SP- set. Red color: *AS* GA SP - set.

The temporal pulse length of the pulse emitted by the transducer can be influenced by the characteristics of the backing element. The backing element is a high density and highly attenuative material that is used to absorb the energy radiating from the back face of the piezoceramic, and controls its vibration. This pulse length is closely related with the transducer bandwidth. The shorter the pulse duration (or length), the larger the bandwidth of the transducer and this can be achieved by the backing effect.

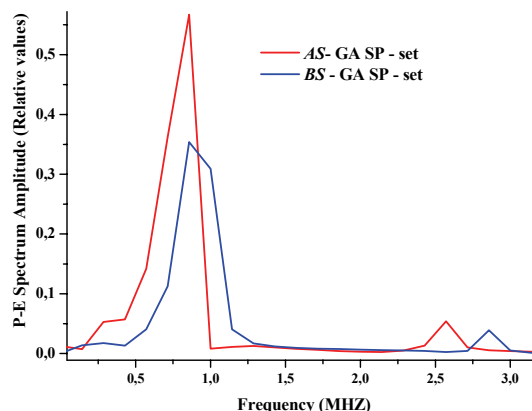


Figure 6: Simulated pulse-echo frequency responses. Blue color: *BS* GA SP- set. Red color: *AS* GA SP-set.

7. SUMMARY AND CONCLUSIONS

Improvements in GA procedure for estimation of constructional parameters in wideband piezoelectric transducers have been presented using a model based on the matrix representation of the piezoelectric transmitter topology. The procedure has been applied to the estimation of four unknown internal parameters, considering up to 1350 possible designs resulting from different GA parameters.

A metric, based on the euclidean distance, was introduced and applied in order to analyze different ultrasonic responses between groups of estimated parameters associated to GA SP sets selected by means this index.

A pulse-echo (P-E) circuitual modeling approach to evaluate practical effectiveness of the different sets of solutions, obtained from the GA procedure and the metric employment, have been presented and applied.

The analysis of several P-E simulated responses in time-frequency domains, allowed clear differences between models with different TP-sets to be established from the point of view of the transducer design, although having similar estimated performance.

The necessity and usefulness of complementing the analysis of the different GA estimation solutions with modelling and simulation tasks was shown. This can help to achieve a better understanding of some physical phenomena involved in the design and functioning of the wideband ultrasonic transducers.

ACKNOWLEDGMENTS

This work was supported by the R&D National Plan of the Spanish Ministry of Education & Science (Project PN DPI2005-00124).

REFERENCES

- Smits J.G., 1976. Iterative method for accurate determination of the real and imaginary parts of the materials coefficients of piezoelectric ceramics, *IEEE Trans. on Son. and Ultrason.*, SU-23 (6), 393-402

- Ruíz, A., San Emeterio, J. L., Ramos, A., 2004. Evaluation of piezoelectric resonator parameters using an artificial intelligence technique. *Integrated Ferroelectrics*, 63, 137-141.
- Capineri L., Masotti L., Rinieri M., and Rocchi S., 1993, Ultrasonic transducer as a black-box: Equivalent circuit synthesis and matching network design. *IEEE Trans. Ultrason., Ferroelect., Freq. Cont.*, 40 (6), 694-703.
- Lockwood G.R., Foster F.S., 2000. Modeling and optimization of High-Frequency ultrasound transducers. *IEEE Trans. Ultrason., Ferroelect., Freq. Cont.*, 41 (2), 826-835
- Ruíz A., Ramos A., San Emeterio J. L., 2004. Estimation of some transducer parameters in a broadband piezoelectric transmitter by using an artificial intelligence technique, *Ultrasonics*, 42, 459-463.
- Goldberg D.E., 1989. Genetic Algorithms in Search, Optimization and Machine Learning. Cambridge, MA: Addison-Wesley
- Krimholtz R., Leedom F., and Matthaei G., 1970. New Equivalent Circuits for Elementary Piezoelectric Transducers, *Electronics Letters*, 6 (13), 398-399
- Orcad™, Beaverton, OR USA. Available from: (www.orcad.com)
- Redwood, M. 1961. Transient Performance of a Piezoelectric Transducer. *J. Acoustic. Soc. Amer.*, 33 (4), 527-536.
- Ramos A., Ruíz A., San Emeterio J. L., Sanz P.T., 2006. PSpice Circuitual Modelling of Ultrasonic Imaging Transceivers including Frequency-dependent Acoustic Losses and Signal Distortions in Electronic Stages, *Ultrasonics*, 44, e995–e1000.
- Ruíz A., Hernández M., Jiménez A., Sotomayor A., Sánchez O., Ramos A., Sanz P. T., J. L. San Emeterio, 2002. Approaches to simulate temporal responses in piezoelectric stages involved in pulsed ultrasonic sensor/actuator systems, *Ferroelectrics*, 273, 243-248.
- Ramos A., San Emeterio J. L., Sanz P.T, 2000. Dependence of pulser driving responses on electrical and motional characteristics of NDE ultrasonic probes, *Ultrasonics*, 38, 553-558.